

## MEASUREMENT OF ILLITE PARTICLE THICKNESS USING A DIRECT FOURIER TRANSFORM OF SMALL-ANGLE X-RAY SCATTERING DATA

CHAO SHANG<sup>1,†</sup>, JAMES A. RICE<sup>1,\*</sup>, DENNIS D. EBERL<sup>2</sup> AND JAR-SHYONG LIN<sup>3</sup>

<sup>1</sup> Department of Chemistry and Biochemistry, South Dakota State University, Brookings, SD 57007, USA

<sup>2</sup> US Geological Survey, Suite E-123, 215 Marine Street, Boulder, CO 80303, USA

<sup>3</sup> Solid State Division, Ridge National Laboratory, Oak Ridge, TN 37831, USA

**Abstract**—It has been suggested that interstratified illite-smectite (I-S) minerals are composed of aggregates of fundamental particles. Many attempts have been made to measure the thickness of such fundamental particles, but each of the methods used suffers from its own limitations and uncertainties. Small-angle X-ray scattering (SAXS) can be used to measure the thickness of particles that scatter X-rays coherently. We used SAXS to study suspensions of Na-rectorite and other illites with varying proportions of smectite. The scattering intensity ( $I$ ) was recorded as a function of the scattering vector,  $q = (4\pi/\lambda) \sin(\theta/2)$ , where  $\lambda$  is the X-ray wavelength and  $\theta$  is the scattering angle. The experimental data were treated with a direct Fourier transform to obtain the pair distance distribution function (PDDF) that was then used to determine the thickness of illite particles. The Guinier and Porod extrapolations were used to obtain the scattering intensity beyond the experimental  $q$ , and the effects of such extrapolations on the PDDF were examined. The thickness of independent rectorite particles (used as a reference mineral) is 18.3 Å. The SAXS results are compared with those obtained by X-ray diffraction peak broadening methods. It was found that the power-law exponent ( $\alpha$ ) obtained by fitting the data in the region of  $q = 0.1$ – $0.6$  nm<sup>-1</sup> to the power law ( $I = I_0 q^{-\alpha}$ ) is a linear function of illite particle thickness. Therefore, illite particle thickness could be predicted by the linear relationship as long as the thickness is within the limit where  $\alpha < 4.0$ .

**Key Words**—Direct Fourier Transform, Illite, Fundamental Particle, Particle Thickness, SAXS.

### INTRODUCTION

Interstratified illite-smectite (I-S) clay particles are common in soils and sediments (Sawhney, 1989; Lindgreen *et al.*, 1991; Laird and Nater, 1993). The stacking structures of these mixed-layer crystallites not only determine their physical-chemical properties, but also reveal the geological history of the environment in which they are present (Środoń *et al.*, 1986; Laird *et al.*, 1991; Jaboyedoff *et al.*, 2000). Based on X-ray diffraction (XRD) characterizations, the particle stacking structures have been described as MacEwan and fundamental particles (Figure 1), *i.e.* the MacEwan particles are formed by stacking fundamental particles (Nadeau *et al.*, 1984; Eberl *et al.*, 1998; Jaboyedoff *et al.*, 2000).

As illustrated in Figure 1, characterizing an I-S mineral involves measuring the number and distribution of illite layers per MacEwan particle, determining the clay's expandability (% smectite layers), and finding the thickness distribution of fundamental particles (or number of mica layers per fundamental particle) (Eberl *et al.*, 1998; Jaboyedoff *et al.*, 2000). Jaboyedoff *et al.* (2001) reported that a quantitative relationship could be established between these particle properties and the

Kübler Index, which is a classical measurement for describing illite crystallinity that is used widely in the petroleum industry. A direct approach for measuring the fundamental particle thickness is to use various microscopic methods (Nadeau *et al.*, 1984; Lindgreen *et al.*, 1991; Środoń *et al.*, 1992; Uhlík *et al.*, 2000), but these methods are time consuming and are able to characterize only a small fraction of the total particle population. A more routine method is to measure the XRD broadening, which is related to the thickness of the coherent scattering domain (CSD) or MacEwan crystallites by applying the Scherrer equation (Drits *et al.*, 1997; Jaboyedoff *et al.*, 1999) or the Bertaut-Warren-Averbach (BWA) method (Drits *et al.*, 1998; Eberl *et al.*, 1998). In the modified form of the Scherrer equation, the usual Scherrer constant (0.89) is replaced with a function that describes the change in the 'constant' with crystal thickness distribution shape. The usual Scherrer constant is applicable only in the particular case when CSDs have a single thickness (Drits *et al.*, 1997). The BWA method is based on Fourier analysis of interference functions for  $00l$  reflections. A computer program (MudMaster; Eberl *et al.*, 1996) is used to remove the Lorentz polarization factor ( $L_p$ ) and the layer scattering intensity ( $G^2$ ) (Drits *et al.*, 1998). Both methods use K-saturated, dehydrated I-S. The thickness of fundamental particles can be calculated from the CSD thickness and the expandability that can be estimated from peak positions of 002/003 reflections of glycolated samples (Drits *et al.*, 1997). For an improvement, Eberl

\* E-mail address of corresponding author:

james\_rice@sdstate.edu

<sup>†</sup>Current address: Department of Crop and Soil Environmental Sciences, Virginia Polytechnic Institute and State University, Blacksburg, VA 24061, USA  
DOI: 10.1346/CCMN.2003.0510305

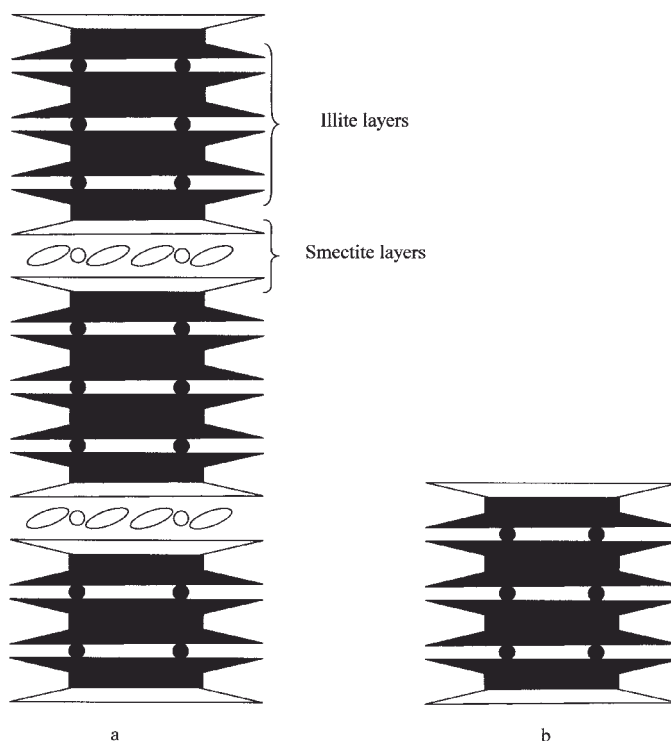


Figure 1. Illustration of (a) MacEwan and (b) fundamental particles.

*et al.* (1998) intercalated Na-saturated I-S with polyvinylpyrrolidone (PVP-10) to eliminate the swelling and then measured the thickness of fundamental illite particles that are approximately  $\geq 2$  nm. The same treatment was also used in a study of mixed-layer clays with high-resolution transmission electron microscopy (HRTEM) (Uhlík *et al.*, 2000; Dudek *et al.*, 2002).

Small-angle X-ray scattering is useful for studying structures that are large, compared with the wavelengths of the scattered radiation (Schmidt, 1995). The scattered intensity is usually expressed in terms of the scattering vector,  $q$ , where  $q = (4\pi/\lambda) \sin(\theta/2)$ ,  $\lambda$  is the X-ray wavelength, and  $\theta$  is the scattering angle which is twice the Bragg angle. Small-angle X-ray scattering can be used to measure the averaged thickness of clay particles which are suspended in water (Shang *et al.*, 2001). Unlike XRD methods, which indirectly give the thickness of fundamental particles, this measurement gives the direct thickness, averaged over millions of particles, and is free of interparticle diffraction. The theory and data treatments for this method are considerably simplified, as compared with the XRD peak broadening methods. Therefore, SAXS provides an independent confirmation and a simple alternative to the XRD methods.

In this report, we explore the application of a SAXS method for determining the thickness of illite particles using a direct Fourier transform. The results were compared with those from the XRD methods (Drits *et al.*, 1997, 1998; Eberl *et al.*, 1998).

## SAXS THEORY

For a thin-layer particle such as a 2:1 aluminosilicate with two dimensions ( $D$ ) that are far larger than the thickness ( $T$ ), the scattering intensity can be written as a cosine-Fourier transform of the pair distance distribution function (PDDF) of particle thickness (Glatter, 1982):

$$I(q) = 4\pi A \int_0^\infty (1/q^2) P_t(r) \cos(qr) dr \quad (1)$$

where  $I(q)$  is experimental scattering intensity,  $A$  is the cross-section area,  $P_t(r)$  is the PDDF and  $r$  is the distance between any two points on a particle. The inverse Fourier transformation of equation 2 gives:

$$P_t(r) = 1/\pi \int_0^\infty I_t(q) \cos(qr) dq \quad (2)$$

where  $I_t(q) = I(q)q^2/(2\pi A)$ .  $I_t(q)$  is the particle cross-section scattering intensity.  $P_t(r) = 0$  when  $r \geq T_{\max}$ , where  $T_{\max}$  is the maximum thickness of clay layer. For a thin-layer particle with homogeneous electron density distribution, the PDDF displays the shape given in Figure 2. The thickness of the particle can then be determined from the PDDF curve that can be constructed by applying equation 2 to the SAXS data. The thickness obtained is an average over  $\sim 10^6$  particles, and the particle thickness distribution, therefore, will apparently affect the results.

Because of instrumental design limitations, a scattering experiment is often conducted over a limited range of scattering vector ( $q_{\min}$  to  $q_{\max}$ ). In the numerical evaluation, equation 2 becomes

$$P_t(r) = 1/\pi \left\{ \int_0^{q_{\min}} I_t(q) \cos(qr) dq + \int_{q_{\min}}^{q_{\max}} I_t(q) \cos(qr) dq + \int_{q_{\max}}^{\infty} I_t(q) \cos(qr) dq \right\} \quad (3)$$

The data for the first and third integrals are not available experimentally; therefore, extrapolations are usually needed for the numerical solution. For the first integral, the Guinier approximation is used; for the third integral, Porod's law is used. The Guinier approximation (Porod, 1982) states that:

$$I_t(q) = I_t(0) \exp(-q^2 R_g^2) \quad (4)$$

where  $I_t(0)$  is the extrapolated  $I$  at  $q = 0$ , and  $R_g$  is the radius of gyration for the particle thickness. At the large- $q$  limit, the Porod law gives:  $I_t(q) \propto q^{-2}$  as  $q \rightarrow \infty$  since  $I(q) \propto q^{-4}$  as  $q \rightarrow \infty$  for the whole particle (Porod, 1982).

The theory and experimental details for the XRD-BWA and Sherrer-equation methods were given by Drits *et al.* (1997, 1998) and Eberl *et al.* (1996, 1998). Some of the results cited in the following text can be obtained from these publications.

## EXPERIMENTAL

Rectorite, a regularly interstratified mica-smectite, was purchased from the Source Clay Minerals Repository, University of Missouri-Columbia, Missouri. The structure of this mineral has been well studied and established by XRD (Bradley, 1950; Kodama, 1966; Henderson, 1970); therefore, it can serve as a reference to test the validity of the SAXS method. Other illites with varying proportions of smectite layers (DV5, Marblehead, RM30 and SG4) were studied previously, and their mean thickness was determined by XRD methods (Eberl *et al.*, 1987; Drits *et al.*, 1997; Drits *et al.*, 1998; Eberl *et al.*, 1998).

The illite samples (DV5 and rectorite) were treated according to the procedure described previously (Shang *et al.*, 2001). Briefly, clay samples were treated with a pH 5 acetate buffer to remove carbonates, hydrogen

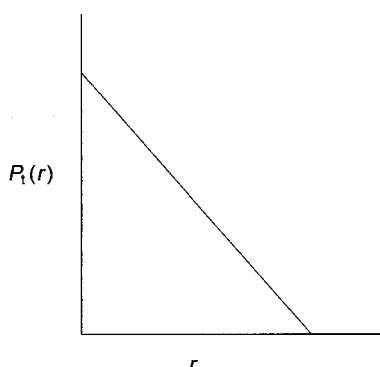


Figure 2. Schematic representation of the PDDF of lamellae with an homogeneous electron distribution.

peroxide (30%) to oxidize organic matter, and dithionite in citrate-bicarbonate buffer to remove free Fe oxides. The treated sample was then shaken with 1 M NaCl to prepare a Na-saturated clay. Excess salts were washed out of the sample with distilled-deionized water using centrifugation, followed by dialysis until a silver nitrate test was negative. The  $<0.1 \mu\text{m}$  and  $0.1-1.5 \mu\text{m}$  fractions in dilute suspension were obtained by centrifugation (CRU-5000, IEC), and the clay suspensions were concentrated on a rotary evaporator to produce concentrated clay stocks, from which a series of samples with the desired clay concentrations were prepared for the scattering study. The concentrations of clay stocks were determined by oven drying a known volume of the clay suspension at  $110^\circ\text{C}$  and weighing.

For SAXS experiments, the particle concentration of rectorite samples ranged from 0.5 to 5%, w/w, and that of DV5 illite ranged from 1 to 5% w/w. The Na-saturated and  $<2 \mu\text{m}$  Marblehead, RM30 and SG4 illites were prepared as described previously for the XRD examination (Drits *et al.*, 1997). To further minimize the sample polydispersity, the  $<1 \mu\text{m}$  fraction was isolated for the SAXS study.

The SAXS measurements were performed with the 10 m SAXS camera at Oak Ridge National Laboratory, Oak Ridge, Tennessee. Wignall *et al.* (1990) described this instrument in detail. Briefly, the 10 m SAXS camera utilizes CuK $\alpha$  radiation ( $\lambda = 0.154 \text{ nm}$ ), point collimation and a two-dimensional position-sensitive detector. The distance between the sample and the detector was 1.119 m for the large- $q$  region measurements (0.18 to  $4.5 \text{ nm}^{-1}$ ) and 5.119 m for the small- $q$  region (0.053 to  $0.9 \text{ nm}^{-1}$ ). Samples were mounted in a metal cell with Kapton windows having a 1 cm internal diameter and 1 mm thickness. The sensitivity of the detector was standardized against Fe-55, and the absolute scattering intensity was obtained by calibration with secondary PES-3 and vitreous carbon standards. Pure water was scanned for background subtraction for dilute samples; for concentrated samples, a Porod plot ( $Iq^4$  vs.  $q^4$ ) was used to find the background scattering.

## RESULTS AND DISCUSSION

Because a dispersed system is a prerequisite for using equation 2 to find  $P_t(r)$  (Porod, 1982), it is important to establish the fact that the reference rectorite particles scatter independently in suspension. Previous studies have shown that the interstratified smectite layers of rectorite exhibit swelling similar to free smectite layers (Kodama, 1966; Henderson, 1970). Thus, with limited knowledge of this mineral's colloidal behavior, there is good reason to suspect that the interlayer interactions might prevent complete particle dispersion.

The scattering behavior of two rectorite suspensions is given in Figure 3. The results show that the scattering curves follow a power-law decay, i.e.  $I(q) \propto q^{-\alpha}$ .

Table 1. The thickness of mineral particles obtained by XRD and SAXS and the  $\alpha$  value of their SAXS power functions.

Mineral sample	$\alpha$ $q = 0.1 - 0.6 \text{ nm}^{-1}$	Thickness by XRD (nm)	Thickness by SAXS (nm)
Laponite	2.05	0.94	
Montmorillonite	2.07	0.94	
IMV smectite	2.91	0.94	
Rectorite ( $<2 \mu\text{m}$ )		1.92	
Rectorite ( $<0.1 \mu\text{m}$ )	2.19		1.83
Rectorite ( $0.1 - 0.15 \mu\text{m}$ )	2.19		1.83
DV5 ( $<2 \mu\text{m}$ )		2.7	
DV5 ( $<0.1 \mu\text{m}$ )	2.27		2.2
DV5 ( $0.1 - 0.15 \mu\text{m}$ )	2.33		2.8
Marblehead	2.99	5.7	5.2
RM30	3.48	12.7	9.5
SG4	4.03	19.2	17.5

In the IMV-smectite sample, particles were present as quasi-crystals. The XRD-thickness values were taken from previous reports (Drits *et al.*, 1997, 1998; Eberl *et al.*, 1996, 1998).

According to Schmidt (1995), systems of independently scattering thin-layer particles should display a scattering curve with  $\alpha = 2.0$ , and a particle with smooth surface will give  $\alpha = 4.0$ . Table 1 gives the  $\alpha$  values for the scattering curves corresponding to  $q = 0.1$  to  $0.6 \text{ nm}^{-1}$  for the illites in this study and the smectites from our other studies (Shang *et al.*, 2001; Shang and Rice, 2003; authors' unpublished data). The  $\alpha$  value increases with increasing particle thickness, ranging from 2.0 for dispersed smectites to 4.0 for SG4 illite. This means that under the SAXS characterization length scale used in this study, illite particles deviate from a thin-layer geometry with increasing particle thickness.

The  $\alpha$  value also becomes larger when the thin-layer smectite particles form quasi-crystals suggesting that the size of quasi-crystals affects the  $\alpha$  value as particle thickness increases (Table 1). Interparticle scattering, caused by high particle concentrations, may also change scattering patterns in the low- $q$  region and thus the  $\alpha$  value (Shang *et al.*, 2001; Shang and Rice, 2003). The

experimental  $\alpha$  value for rectorite, however, remains constant for a wide range of particle concentrations (0.5–5% w/w). Rectorite's higher  $\alpha$  value (2.19) compared to that of montmorillonite (2.07) (Table 1) can be attributed to the thickness factor. Therefore, we conclude that the Na-saturated rectorite is present in water as independent particles, particularly in low particle concentrations (0.5–1%). The two size-fractions of rectorite have the same  $\alpha$  value suggesting that the size fractionation (between  $<0.1$  and  $0.1 - 0.15 \mu\text{m}$ ) is not related to the particle thickness. In other words, rectorite samples have a uniform thickness distribution (monodisperse with respect to particle thickness). These results validate the use of this mineral as a reference for testing the accuracy of SAXS to measure the thickness of other illite samples.

Figure 4 shows the PDDF for the  $<0.1 \mu\text{m}$  rectorite in a 1% suspension. Although the PDDF does not converge to zero, its linearity allows extrapolation for the determination of particle thickness. The extrapolated

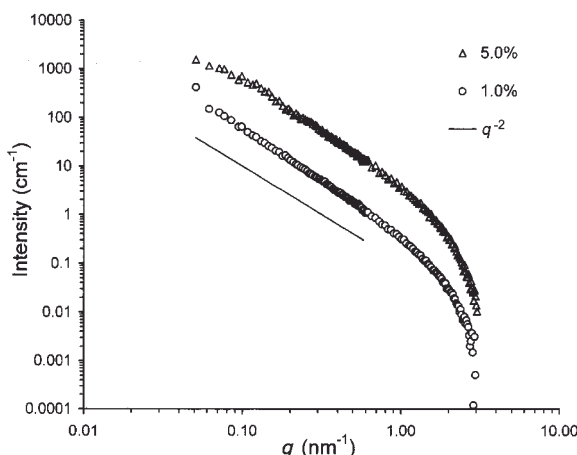


Figure 3. The SAXS results for  $<0.1 \mu\text{m}$  rectorite suspensions of two particle concentrations.

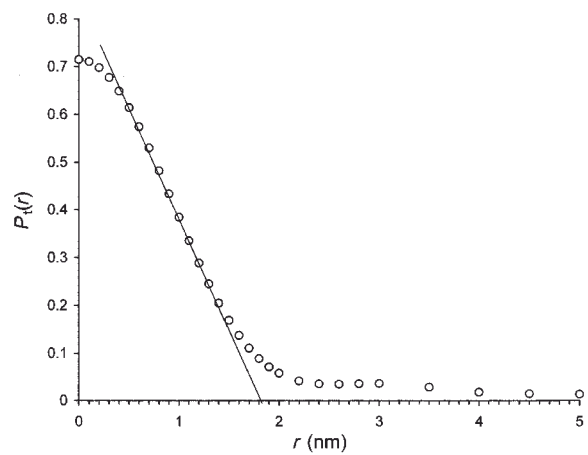


Figure 4. PDDF calculated from the SAXS data for 1% rectorite of  $<0.1 \mu\text{m}$ .

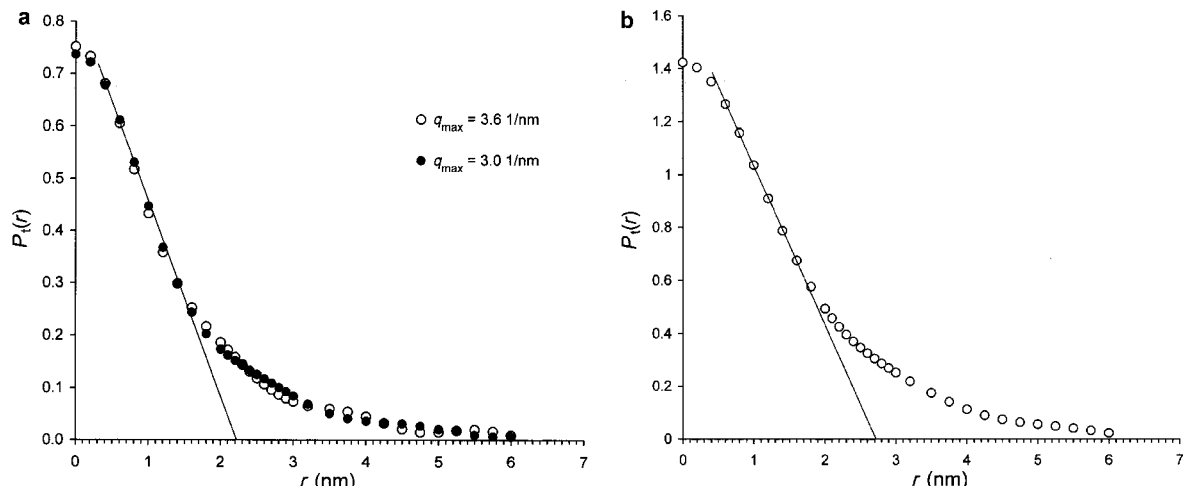


Figure 5. PDDF calculated from the SAXS data for (a) the  $<0.1\text{ }\mu\text{m}$  fraction of 1% DV5, and (b) the  $0.1\text{--}0.15\text{ }\mu\text{m}$  fraction.

thickness is 1.83 nm, which is smaller than 1.92 nm that was obtained by XRD (Bradley, 1950). The difference could be attributed to experimental error and the saturated cations that occupy the interlayer space. The two size-fractions gave an identical thickness (Table 1). This confirms the previous conclusion based on the analysis of value observations.

The PDDFs for the  $<0.1\text{ }\mu\text{m}$  and  $0.1\text{--}0.15\text{ }\mu\text{m}$  fractions of DV5 are given in Figure 5. The particle thickness of  $<0.1\text{ }\mu\text{m}$  is 2.2 nm and that for  $0.1\text{--}0.15\text{ }\mu\text{m}$  is 2.8 nm, compared with a value of 2.7 nm for the  $<2\text{ }\mu\text{m}$  fraction by the XRD method (Table 1). In both cases, extrapolation to the  $x$ -axis is needed to determine the particle thickness because of non-zero convergence. There could be several factors contributing to the non-zero convergence at the distance axis: the variation in particle thickness (*i.e.* polydispersity), limited extrapolation of  $I(q)$  data beyond the experimental range, interparticle interactions through diffuse double layers, instrument-related statistical errors, *etc.* The variation in the thickness is in agreement with the  $\alpha$  values shown in Table 1, *i.e.* the coarse fraction contains thicker particles suggesting a particle-thickness polydispersity, which could be significant even within a size-fraction. We speculate that the particle-thickness polydispersity has contributed to the poor convergence of the PDDF (Figure 5), when it is compared with the PDDF of rectorite that has particle thickness monodispersity and a better convergence in the PDDF (Figure 4). In many independent-particle systems, scattering in the large- $q$  region usually contains significant noise resulting from solvent scattering, and this uncertainty may affect the shape of the PDDF. This hypothesis was tested by removing a portion of scattering data from the large- $q$  region of the scattering data ( $q$  from  $3.0\text{ nm}^{-1}$  to  $3.6\text{ nm}^{-1}$  in this case). This treatment slightly reduced the oscillation at the tail portion of the PDDF but did not improve the convergence (Figure 5a).

The effect of  $I(q)$  extrapolation on the PDDF was also tested using the RM30 scattering data. The PDDF without the Guinier extrapolation oscillates along the distance axis and is not useful for thickness determination (Figure 6a). Extrapolating  $I(q)$  to  $q = 10\text{ nm}^{-1}$  did not improve the PDDF. However, this oscillation can be removed by Guinier extrapolation to  $q = 10^{-4}\text{ nm}^{-1}$  (Figure 6b). Using this extrapolation, the RM30 particle thickness is estimated to be 9.5 nm (Figure 6b) which is close to the value of 9.2 nm determined by HRTEM (Dudek *et al.*, 2002). By XRD methods it has been estimated to be 12.9 nm (Table 1) though a wide variation exists among reported values (Drits *et al.*, 1997, 1998; Eberl *et al.*, 1998). Carlson and Schmidt (1969) demonstrated that the oscillation of the PDDF obtained from a direct Fourier transform was so severe that determining the dimension of scattering particles was essentially impossible. This is one of the factors that make mathematical modeling and the indirect Fourier transform more attractive in deriving the dimensions of scattering particles using small-angle scattering data (Glatter, 1982, 1995).

The particle thickness values for the Marblehead and SG4 illites are also given in Table 1. It appears that compared to the thicknesses obtained by XRD methods, SAXS data underestimate the particle thickness. The difference between the two methods is more significant for thicker illite particles. However, the thickness for SG4 by SAXS is close to that obtained by TEM (17.8 nm). Eberl *et al.* (1998) argued that TEM seems to generally give smaller thickness estimates. Because of the polydispersity of the samples, the particles in the  $<1\text{ }\mu\text{m}$  fractions studied should, presumably, be thinner than those in the  $<2\text{ }\mu\text{m}$  fractions used by the XRD methods. It appears that a more extensive size fractionation would be required to reduce the polydispersity of the samples in order to improve the accuracy of the SAXS measurements.

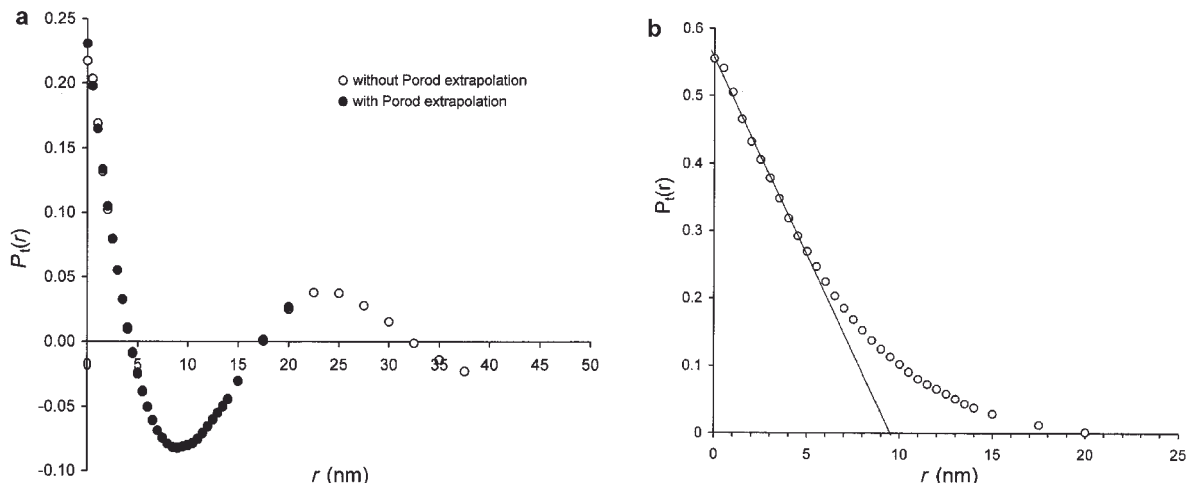


Figure 6. Effects of extrapolation in (a) the Porod region and (b) the Guinier region on the PDDF obtained from SAXS data for RM30.

In this study, the I-S fundamental particles are clearly operationally defined; the smectite layers in the Na (or Li) form are dispersible in water, so MacEwan particles are dispersed into fundamental particles. Thus, the thickness of a fundamental particle is the distance between the two smectite layers (Figure 1). Because the particles studied are in a dispersed state (cleavage of the particles was not tested), the definition used here does not embody all elements of the fundamental particle concept as proposed by Nadeau *et al.* (1984) for interpreting the XRD and TEM results of I-S minerals. The practical significance of Nadeau's proposal has been disputed because interparticle diffraction may occur in fine size-fractions (Kasama *et al.*, 2001), and because the stacking pattern in an oriented sample does not necessarily represent the natural stacking of the mineral in a rock (Peacor, 1998).

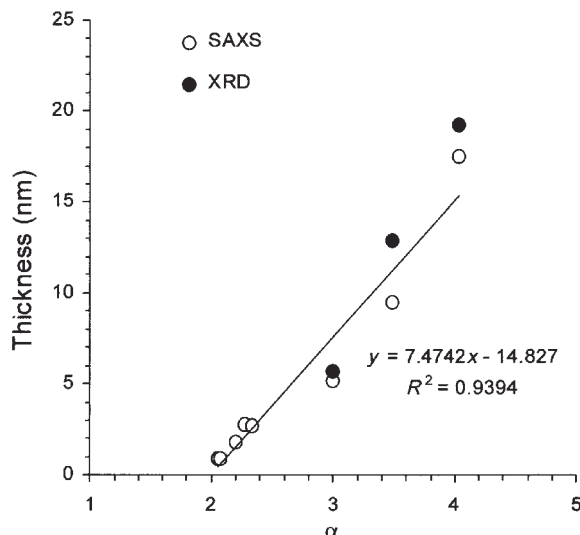


Figure 7. Relationship between the exponent of power-law scattering function ( $\alpha$ ) and the particle thickness.

With the SAXS thickness available, it is of interest to re-examine the relationship between the  $\alpha$  value and the particle thickness. Figure 7 shows that this relationship is linear; therefore, the thickness for an unknown sample can be reasonably predicted as long as it is below the thickness limit  $\alpha = 4$ . Above this limit, all fundamental particles scatter as a smooth surface. The linear relationship between the  $\alpha$  value and the particle thickness reminds us of the need for the careful use of the  $\alpha$  value in studying the fractal property of particles in natural environments (Dékány *et al.*, 1994, 1999). According to Schmidt (1995),  $1 \leq D_m < 3$  for  $\alpha < 3$ ; for  $3 < \alpha \leq 4$ ,  $D_s = 6 - \alpha$ , and  $2 \leq D_s < 3$ ; where  $D_m$  and  $D_s$  are mass and surface fractal dimensions, respectively. For example,  $\alpha = 2.91$  for a flocculated smectite system, compared with 2.07 for a dispersed system (Table 1); the system therefore exhibits a mass fractal nature with  $D_m = 2.91$ . Thus, it is evident that the contribution to the  $\alpha$  value from the fundamental particle thickness should also be considered when dealing with interparticle interactions.

## CONCLUSIONS

We have successfully applied SAXS in combination with a direct Fourier transform to determine the thickness of illite particles. The method has avoided the interparticle diffraction encountered in XRD methods and gives a direct measurement of thickness, averaged over millions of particles. The oscillation in the PDDF caused by limited experimental data in the low- $q$  region of the data set can be removed by a Guinier extrapolation. An excellent agreement was found between the XRD and SAXS methods for determining the thickness value for relatively thin particles, but discrepancies were observed between the two methods when thicker particles were characterized. The convergence of the PDDF became poor for thicker particles.

These problems could be caused by the polydispersity of samples with respect to particle thickness; however, the true reasons require further investigation. The accessible lower limit of the scattering vector ( $q$ ), which is inherently associated with a particular instrument geometry, ultimately determines the upper limit for the thickness that can be measured by SAXS. The use of ultra-small angle X-ray scattering cameras (Morvan *et al.*, 1994; Ando and Konishi, 2000; Levitz *et al.*, 2000), however, will extend the limit to encompass all illite fundamental particle dimensions typically found in nature.

### ACKNOWLEDGMENTS

The project was supported by a grant from the USDA National Research Initiative Competitive Grants program through award number 98-35107-6515. The use of the SAXS facility at Oak Ridge National Laboratory was sponsored in part by the US Department of Energy under Contract No. DE-AC05-00OR22725 with the Oak Ridge National laboratory, managed by the UT-Battelle, LLC.

### REFERENCES

- Ando, H. and Konishi, T. (2000) Structure analysis of regenerated cellulose hydrogels by small-angle and ultra-small-angle X-ray scattering. *Physical Review E*, **62**, Part B, 727–733.
- Bradley, W.F. (1950) The alternating layer sequence of rectorite. *American Mineralogist*, **35**, 590–595.
- Carlson, R.D. and Schmidt, P.W. (1969) Tests of a Hankel transform method of determining electron densities of long cylinders from small angle X-ray scattering data. *Journal of Applied Crystallography*, **2**, 297–300.
- Dékány, I., Szekeres, M., Marosi, T., Balázs, J. and Tombácz, E. (1994) Interaction between ionic surfactants and soil colloids: adsorption, wetting and structural properties. *Progress in Colloid & Polymer Science*, **95**, 73–90.
- Dékány, I., Turi, L., Fonseca, A. and Nagy, J.B. (1999) The structure of acid treated speiolites: small-angle X-ray scattering and multi MAS-NMR investigations. *Applied Clay Science*, **14**, 141–160.
- Drits, V.A., Środoń, J. and Eberl, D.D. (1997) XRD measurement of mean thickness of illite/smectite; reappraisal of the Kübler index and the Scherrer equation. *Clays and Clay Minerals*, **45**, 461–475.
- Drits, V.A., Eberl, D.D. and Środoń, J. (1998) XRD measurement of mean thickness, thickness distribution and strain for illite and illite-smectite crystallites by the Bertaut-Warren-Averbach technique. *Clays and Clay Minerals*, **46**, 38–50.
- Dudek, T., Środoń, J., Eberl, D.D., Elsass, F. and Uhlik, P. (2002) Thickness distribution of illite crystals in shales. I: X-ray diffraction vs. high-resolution transmission electron microscopy measurements. *Clays and Clay Minerals*, **50**, 562–577.
- Eberl, D.D., Środoń, J., Lee, M., Nadeau, P.H. and Northrop, H.R. (1987) Sericite from the Silverton caldera, Colorado: Correlation among structure, composition, origin, and particle thickness. *American Mineralogist*, **72**, 914–934.
- Eberl, D.D., Drits, V.A., Środoń, J. and Nüesch, R. (1996) *MudMaster: A program for calculating crystallite size distributions and strain from the shapes of X-ray diffraction peaks*. US Geological Survey Open File Report **96-171**, 44 pp.
- Eberl, D.D., Nuesch, R., Šuchá, V. and Tsipursky, S. (1998) Measurement of fundamental illite particle thicknesses by X-ray diffraction using PVP-10 intercalation. *Clays and Clay Minerals*, **46**, 89–97.
- Glatter, O. (1982) Data treatment and interpretation. Pp. 119–196 in: *Small-Angle X-ray Scattering* (O. Glatter and O. Kratky, editors). Academic Press, New York.
- Glatter, O. (1995) Modern methods of data analysis in small-angle scattering and light scattering. Pp. 107–180 in: *Modern Aspects of Small-Angle Scattering* (H. Brumberger, editor). Proceedings of the NATO Advanced Study Institutes, Como, Italy, May 1993, Kluwer Academic Publishers, Dordrecht, The Netherlands.
- Henderson, G.V. (1970) The origin of pyrophyllite rectorite in shales of north central Utah. *Clays and Clay Minerals*, **18**, 239–246.
- Jaboyedoff, M., Kübler, B. and Thélin, Ph. (1999) An empirical Scherrer equation for weakly swelling mixed-layer minerals, especially illite-smectite. *Clay Minerals*, **34**, 601–617.
- Jaboyedoff, M., Kübler, B., Sartori, M. and Thélin, Ph. (2000) Basis for meaningful illite crystallinity measurements: an example from the Swiss PreAlps. *Schweizerische Mineralogische und Petrographische Mitteilungen*, **80**, 75–83.
- Jaboyedoff, M., Bussy, F., Kübler, B. and Thélin, Ph. (2001) Illite "crystallinity" revisited. *Clays and Clay Minerals*, **49**, 156–167.
- Kasama, T., Murakami, T., Kohyama, N. and Watanabe, T. (2001) Experimental mixtures of smectite and rectorite: Reinvestigation of 'fundamental particles' and 'interparticle diffraction'. *American Mineralogist*, **86**, 105–114.
- Kodama, H. (1966) The nature of the component layers of rectorite. *American Mineralogist*, **51**, 1035–1055.
- Laird, D.A. and Nater, E.A. (1993) Nature of the illitic phase associated with randomly interstratified smectite/illite in soils. *Clays and Clay Minerals*, **41**, 280–287.
- Laird, D.A., Barak, P., Nater, E.A. and Dowdy, R.H. (1991) Chemistry of smectitic and illitic phases in interstratified soil smectite. *Soil Science Society of America Journal*, **55**, 1499–1504.
- Levitz, P., Lecolier, E., Mourchid, A., Delville, A. and Lyonnard, S. (2000) Liquid-solid transition of laponite suspensions at very low ionic strength: Long-range electrostatic stabilisation of anisotropic colloids. *Europhysics Letters*, **49**, 672–677.
- Lindgreen, H., Garnæs, J., Hansen, P.L., Besenbacher, F., Lægsgaard, E., Stensgaard, I., Gould, S.A.C. and Hansma, P.K. (1991) Ultrafine particles of North sea illite/smectite clay minerals investigated by STM and AFM. *American Mineralogist*, **76**, 1218–1222.
- Morvan, M., Espinat, D., Lambard, J. and Zemb, Th. (1994) Ultrasmall- and small-angle X-ray scattering of smectite clay suspensions. *Colloids and Surfaces A*, **82**, 193–203.
- Nadeau, P.H., Wilson, M.J., McHardy, W.J. and Tait, J.M. (1984) Interstratified clays as fundamental particles. *Science*, **225**, 923–925.
- Peacor, D.R. (1998) Implications of TEM data for the concept of fundamental particles. *The Canadian Mineralogist*, **36**, 1397–1408.
- Porod, G. (1982) General theory. Pp. 17–51 in: *Small-Angle X-ray Scattering* (O. Glatter and O. Kratky, editors). Academic Press, New York.
- Sawhney, B.L. (1989) Interstratification in layer silicates. Pp. 789–828 in: *Minerals in Soil Environments* (J.B. Dixon and S.B. Weed, editors). Soil Science Society of America, Madison, Wisconsin.
- Schmidt, P.W. (1995) Some fundamental concepts and techniques useful in small-angle scattering studies of disordered solids. Pp. 1–56 in: *Modern Aspects of Small-Angle Scattering* (H. Brumberger, editor). Proceedings of

- the NATO Advanced Study Institutes, Como, Italy, May 1993, Kluwer Academic Publishers, Dordrecht, The Netherlands.
- Shang, C. and Rice, J.A. (2003) Invalidity in deriving inter-particle distance in clay-water systems using the experimental structure factor maximum obtained by small-angle scattering. *Langmuir* (submitted).
- Shang, C., Rice, J.A. and Lin, J.S. (2001) Thickness and surface characteristics of colloidal 2:1 aluminosilicates using indirect Fourier transform of small-angle X-ray scattering data. *Clays and Clay Minerals*, **49**, 277–282.
- Środoń, J., Morgan, D.J., Eslinger, E.V., Eberl, D.D. and Karlinger, M.K. (1986) Chemistry of illite/smectite and end-member illite. *Clays and Clay Minerals*, **34**, 368–378.
- Środoń, J., Elsass, F., McHardy, W.J. and Morgan, D.J. (1992) Chemistry of illite-smectite inferred from TEM measurements of fundamental particles. *Clay Minerals*, **27**, 137–158.
- Uhlík, P., Šuchá, V., Elsass, F. and Čaplovíčová, M. (2000) High-resolution transmission electron microscopy of mixed-layer clays dispersed in PVP-10: a new technique to distinguish detrital and authigenic illitic material. *Clay Minerals*, **35**, 781–189.
- Wignall, G.D., Lin, J.S. and Spooner, S. (1990) The reduction of parasitic scattering in small-angle X-ray scattering by three pinhole collimating system. *Journal of Applied Crystallography*, **23**, 241–246.

(Received 7 May 2002; revised 3 January 2003; Ms. 656; A.E. Peter J. Heaney)